BMC Plant Biology

RESEARCH

Open Access

# Evaluation of the molecular mechanism underlying proline metabolic and catabolic pathways and some morpho-physiological traits of tobacco (*Nicotiana tabacum* L.) plants under arsenic stress

Nader Adamipour[1], Farzad Nazari[1*], Ayoub Molaahmad Nalousi[1] and Jaime A. Teixeira da Silva[2]

## Abstract

**Background** In recent decades, arsenic (As) toxicity has emerged as a significant challenge in many countries. It not only reduces the growth and performance of plants, but also poses a threat to human health. The synthesis of compatible solutes, particularly proline, is a mechanism plants utilize to cope with stress. Investigating the metabolic pathways of proline would deepen our understanding for future molecular breeding or genetic engineering efforts. Therefore, the aim of this study was to explore the metabolic and catabolic pathways of proline, as well as the morpho-physiological traits of tobacco, under As stress.

**Results** The results revealed a significant decrease in morphological traits and photosynthetic efficiency, chlorophyll content, and total soluble protein content with increasing As concentration. The results also showed that proline content, total soluble carbohydrates, hydrogen peroxide, and malondialdehyde, as well as the activity of two antioxidant enzymes, superoxide dismutase and ascorbate peroxidase, increased with increasing As concentration. At 10 mg As $Kg^{-1}$ soil, the expression of $\Delta^1$-pyrroline-carboxylate synthetase (*P5CS*) and P5C reductase (*P5CR*) genes was not different from the control, but their expression increased significantly at 20 and 40 mg As $Kg^{-1}$ soil. At 10 mg As $Kg^{-1}$ soil, the expression of proline dehydrogenase (*PDH*) and P5C dehydrogenase (*P5CDH*) genes decreased sharply compared to the control but remained unchanged at 20 and 40 mg As $Kg^{-1}$ soil. At 10 and 20 mg As $Kg^{-1}$ soil, expression of the ornithine δ-aminotransferase (*OAT*) gene was unchanged compared to the control, but at 40 mg As $Kg^{-1}$ soil, it increased sharply.

**Conclusion** The results showed that the accumulation of proline at the lowest (10 mg As $Kg^{-1}$ soil) tested As concentration was due to a decrease in the expression of proline catabolic genes (*PDH* and *P5CDH*), while the genes involved in proline synthesis did not play a role. At 20 mg As $Kg^{-1}$ soil, proline accumulation was caused by the increased expression of genes (*P5CS* and *P5CR*) involved in the glutamate pathway of proline synthesis. Additionally, at the highest concentration of arsenic (40 mg As $Kg^{-1}$ soil), the *OAT* gene, which is active in the ornithine pathway, was also involved in proline synthesis, along with the *P5CS* and *P5CR* genes.

*Correspondence:
Farzad Nazari
f.nazari@uok.ac.ir
Full list of author information is available at the end of the article

**Keywords** Abiotic stress, Amino acids, Compatible solutes, Gene expression, Heavy metals

## Introduction

During their growth, plants are constantly challenged by unfavorable environmental conditions such as biotic and abiotic stresses [1]. Heavy metal stress is an abiotic stress that significantly impacts plant growth and performance by altering various biochemical responses [2]. Heavy metals are metallic elements that are toxic or poisonous at low concentrations, or metals and metalloids with an atomic density > 4 g $cm^{-3}$ [3].

Arsenic (As) is one of the heavy metals that is harmful to plants, animals, and humans, and according to the World Health Organization (WHO), the level of As in drinking water should not exceed 10 μg $L^{-1}$ [4, 5]. Its accumulation in food products can pose a risk to human health. Data published by the Agency for Toxic Substances and Disease Registry shows that As is ranked first in terms of its toxicity to humans [6]. Over 200 million people in 105 countries are exposed to As concentrations that exceed the permissible limit recommended by the WHO and, according to the International Agency of Research on Cancer, As is classified as a class-1 carcinogen [7].

As naturally enters the food chain through the degradation of minerals by microorganisms [8]. In addition, human activities such as mining, copper smelting, coal combustion, use of pesticides, herbicides, wood preservatives, and irrigation with As-contaminated groundwater are other sources of As contamination [6, 9, 10]. As is not an essential element for plants, but the exposure of roots to As can inhibit their growth and expansion due to reduced cell division and expansion [11–13]. As toxicity in plants can lead to multiple negative responses to their growth and physiology, including reduced germination, impaired energy production, decreased area and number of leaves, wilting and necrosis of leaves, inhibition of respiratory enzymes, inhibition of photosynthetic activity, reduction of nutrition uptake, irregularity in membrane structures, lipid peroxidation, and electrolyte leakage [14]. To cope with heavy metal stress, plants employ a range of strategies, including exclusion, the synthesis of metal-binding polypeptides, the formation of complexes such as metallothioneins and phytochelatins, but plants can also store heavy metals in specific parts of the plant, via compartmentalization, and synthesize compatible solutes in response to them [15, 16]. Compatible solutes, which are organic composites with low molecular weight and high solubility, are typically non-toxic even when they are present at high concentrations within cells [17]. These solutes protect plants against stress by assisting with the stabilization of enzymes or proteins, scavenging free radicals, adjusting of cellular osmosis, and protecting membrane integrity [18, 19]. Quaternary ammonium compounds, polyols, trehalose, sucrose, and proline are some of the most functionally important compatible solutes [20].

Proline is a proteinogenic amino acid that functions as a metal chelator, signaling molecule, excellent osmolyte, and antioxidant defense molecule during environmental stress [21, 22]. The increase in proline content when plants are exposed to stress caused by heavy metals such as As, cadmium (Cd), lead (Pb), copper (Cu), and chromium (Cr) has been reported in wheat (*Triticum aestivum* L.) [23], carrot (*Daucus carota* L.) [24], barley (*Hordeum vulgare* L.) [25], tomato (*Solanum lycopersicum* L.) [26], and mungbean (*Vigna radiata* L.) [27] plants. The accumulation of proline during heavy metal stress prevents the denaturation of enzymes, assists with osmoregulation, regulates cytosolic acidity, stabilizes protein synthesis, scavenges free radicals, and serves as a reservoir of carbon and nitrogen [28, 29]. Proline is synthesized from glutamate and ornithine pathways in plants. The glutamate pathway is found in the cytosol and chloroplasts and consists of two steps [30]. In this pathway, glutamate is reduced to glutamate semialdehyde (GSA) by $\Delta^1$-pyrroline-carboxylate synthetase (P5CS), and GSA is converted to pyrroline-5-carboxylate (P5C), which is then reduced to proline by P5C reductase (P5CR) [31]. Proline can be synthesized from ornithine through an alternative pathway, in which ornithine is first transaminated by ornithine δ-aminotransferase (OAT), producing GSA and P5C, which is then converted to proline [30, 31]. Two enzymes, proline dehydrogenase (PDH) and P5C dehydrogenase (P5CDH), are responsible for proline catabolism in mitochondria. P5CDH and PDH are encoded by one and two genes, respectively [32–34]. Proline is converted to P5C by PDH and then P5C is oxidized to glutamate by P5CDH. If P5C oxidase is disrupted, P5C can enter the cytosol from mitochondria by an unknown transporter and is then reduced to proline by P5CR. However, this metabolic shortcut is unknown in plants and there is limited evidence to either support or refute its existence [31].

Worldwide, tobacco (*Nicotiana tabacum* L.) is a widely recognized economically important crop, and soils contaminated with As not only reduce the yield and growth of this plant but could be transferred to smokers after being absorbed by the plant, with the potential of causing heart diseases and cancer [35]. As toxicity is facing challenges and criticisms in various countries, particularly in regions of Iran where tobacco is cultivated using As-contaminated water [36, 37].

To date, no comprehensive study in plants has reported the proline metabolic pathway under As toxicity.

Therefore, this research was conducted to evaluate the proline pathway, molecular responses, as well as some morpho-physiological traits of tobacco under As stress to strengthen our knowledge of this plant's stress response under As stress, offering critical insight to develop stress-tolerant plants through molecular breeding or genetic engineering.

## Materials and methods

### Experimental site and design

In order to evaluate the effect of As toxicity on the metabolic and catabolic pathways of proline and the morpho-physiological characteristics of tobacco plants, a greenhouse experiment was conducted in a completely randomized design in the greenhouse of the Department of Horticultural Science, University of Kurdistan, Sanandaj, in Iran. As stress was evaluated at four levels: 0.05, 10, 20, and 40 mg As $Kg^{-1}$ soil, with four replications for each level.

### Plant materials, growth conditions, and arsenic treatments

The soil used in the experiment was collected from a depth of 0–30 cm from the research farm of the Faculty of Agriculture at the University of Kurdistan, in Iran (35°16′ E and 46°59′ N). Soil samples were grounded, homogenized, sieved through a 2 mm sieve, and mixed to determine their physicochemical properties (Table 1). Each pot was filled with 2.5 kg of soil. Before filling pots, 2.5 kg of soil was weighed and placed in plastic bags. The required amount of As, in the form of $Na_2HAsO_4.7H_2O$, was calculated based on the treatments of 10, 20, and 40 mg As $Kg^{-1}$ soil and added to the soil where it was mixed evenly. The plastic bags were exposed to successive wet-dry cycles in the greenhouse over 3 months to redistribute the As in soil colloids. To achieve this, soil containing different concentrations of As was brought to 50% field capacity (FC) with water and then allowed to dry by air [38]. No As was added to control soil, although it contained trace amounts of As (0.05 mg As $Kg^{-1}$ soil). After 3 months of storing As-contaminated soils in the greenhouse, the pots (19×13 cm: diameter×height; 3684.01 $cm^3$ volume) were filled with 2.5 kg of soil. In this experiment, pots without drainage were used so that when irrigating the plants, As did not filter out of the bottom of pots along with the water. Therefore, the amount of As in soil remained constant. Two seeds of tobacco cv. Burley 21 (Marivan Tobacco Company, Kurdistan, Iran) were planted in each prepared pot at a depth of 1 cm and kept in a greenhouse. Before planting, seeds were disinfected with 70% (v/v) ethanol for 1 min, followed by 30% (v/v) sodium hypochlorite for 10 min, and then rinsed once with distilled water [39]. When seedlings reached the two-leaf stage, the strongest seedling in each pot was kept while the remaining and weaker seedling was removed. Pots were kept in greenhouse conditions (average day and night temperatures of 24–18 °C, 50–60% relative humidity, 700–900 µmol $m^{-2}$ $s^{-1}$ photosynthetic photon flux density, and 15-h photoperiod) for 50 days. Pots were irrigated every three days to 70% of FC. After 50 days, the whole plant was removed from each pot to perform physiological and molecular analyses. Before removing each plant, two terminal leaves were wrapped in aluminum foil, promptly placed in liquid nitrogen, and stored at −80 °C to measure physiological traits and gene expression.

### Measurements

#### *Morphological traits*

After 50 days, plants were removed from pots, and the soil surrounding roots was carefully washed under running tap water. Root and shoot fresh weight (FW) was recorded immediately. Leaf area was measured using a leaf area meter (WinDIAS 3, Delta-T devices, Cambridge, UK). Shoots and roots were placed in separate envelopes and dried in an electric oven (Heraeus Electric, Hanau, Germany) at 85 °C for 72 h, and then the dry weight (DW) of both shoots and roots was recorded [40].

### Physiological traits

#### *Photosynthetic efficiency*

Four fully grown terminal leaves were used to measure photosynthetic efficiency with a portable photosynthesis meter (miniPPM-100, EARS, Delft, the Netherlands) [41].

#### *Chlorophyll content*

To assess chlorophyll content, 0.5 g of terminal leaves were homogenized in a mortar with 10 mL of 80% (v/v) acetone. The resulting extract was then centrifuged (MIKRO 200, Hettich, Tuttlingen, Germany) at 14,000 g for 5 min. The supernatant was collected, and its

**Table 1** Some physico-chemical properties of soil used in this study

| Field capacity (%) | Permanent wilting point (%) | Sand (%) | Silt (%) | Clay (%) | pH | EC (dS $m^{-1}$) | Organic matter (%) | Arsenic (mg $kg^{-1}$ soil) |
|---|---|---|---|---|---|---|---|---|
| 27 | 6 | 17 | 49 | 34 | 7.2 | 1.2 | 3.01 | 0.05 |

absorbance was read at 663 and 646 nm with a UNICO UV-2100 spectrophotometer (Shanghai, China). Finally, chlorophyll content was determined using the following formula [42]:

$$\text{Total chlorophyll (mg g}^{-1}\text{ FW)} = (20.2 \times A_{646} + 8.02 \times A_{663}) \times V/(W \times 1000)$$

where V is the volume of sample extract and W is sample weight.

## Biochemical traits

### *Total soluble carbohydrates*

To measure the soluble carbohydrates in samples, an established method was used [43]. Briefly, 0.5 g of terminal leaves was crushed into a fine powder using a pestle and liquid nitrogen in a mortar. To each powdered sample, 5 mL of 95% ethanol was added and thoroughly homogenized. Samples were then transferred into 15 mL Falcon tubes (Corning, NY, USA) and centrifuged at 3500 g for 10 min. One mL of the supernatant was mixed with 3 mL of anthrone reagent, which was prepared by dissolving 150 mg of anthrone in 100 mL of 72% sulfuric acid, and incubated in a hot water bath (WNB 45, Memmert, Germany) at 100 °C for 10 min. Upon returning to ambient temperature, absorbance of the samples was recorded at λ = 625 nm. Total soluble carbohydrate content was quantified by a standard curve, which was calibrated with glucose at several concentrations: 0, 20, 40, 60, 80, and 100 mg $L^{-1}$.

### *Total protein content*

Using Bradford's [44] method, the enzyme extract was initially prepared by homogenizing 0.5 g of terminal leaves in 5 mL of 100 mM potassium phosphate buffer (pH 7.0) in a mortar with a pestle. The resulting homogenate was centrifuged at 15,000 g for 20 min. A 100 µL aliquot of the supernatant was mixed with 5 mL of the color reagent, which was prepared as follows: 100 mg of Coomassie Brilliant Blue G-250 was dissolved in 50 mL of 95% ethanol, then 100 mL of 85% orthophosphoric acid ($H_3PO_4$) was added, and the final volume was adjusted to 1000 mL with distilled water. Following brief vortexing, absorbance was measured at 595 nm. Protein content was determined by preparing a standard curve with bovine serum albumin at 0, 10, 20, 40, 60, 80, 100, and 140 mg $L^{-1}$.

### *Proline content*

Following the method established by Bates et al. [45], proline content was assessed as follows: Initially, 0.1 g of terminal leaves tissue was homogenized in 2 mL of 3% sulfosalicylic acid, followed by centrifugation at 10,000 g for 15 min, then 2 mL of the resultant supernatant was added to 2 mL of ninhydrin reagent (1.25 g of ninhydrin was dissolved in a mixture of 30 mL of acetic acid and 20 mL of 6 M phosphoric acid, with the solution being stirred continuously at low heat) and 2 mL of acetic acid. The mixture was heated in a water bath at 100 °C for 1 h, then was promptly cooled on ice. To each sample, 4 mL of toluene was added, followed by vortexing for 30 s. Once the samples had settled, forming distinct phases, absorbance of the upper phase was measured at 520 nm with a spectrophotometer. Proline content was determined from a standard curve prepared with proline standard solutions ranging from 0 to 60 mg $L^{-1}$.

### *Hydrogen peroxide ($H_2O_2$) content*

$H_2O_2$ content was measured using the Cui et al. [46] protocol. In this method, 1 g of terminal leaves was homogenized with 2 mL of 0.1% (w/v) trichloroacetic acid (TCA) in a mortar with a pestle. After centrifuging the homogenate at 12,000 g for 10 min, 500 µL of the supernatant was mixed with 0.5 mL of 10 mM K-phosphate buffer (pH 7.0) and 1 mL of reagent (1 M potassium iodide in freshly double-distilled water). The mixture was incubated in the dark for 1 h, after which absorbance was measured at 390 nm. $H_2O_2$ content was determined from a standard curve prepared with 0, 2, 4, 6, 8, and 10 mg $L^{-1}$ $H_2O_2$.

### *Malondialdehyde (MDA) content*

MDA content was measured using the Li et al. [47] method. At first, 0.2 g of leaf tissue was homogenized in 5 mL of 0.1% (w/v) TCA. The mixture was then centrifuged in a Falcon tube at 10,000 g for 5 min at 4 °C. After centrifugation, 1 mL of the supernatant was mixed with 0.25 mL of 20% (w/v) TCA, 0.25 mL of 0.01% (w/v) butylated hydroxytoluene, and 0.5 mL of 0.65% (w/v) thiobarbituric acid. The mixture was then heated in a water bath at 95 °C for 30 min, then cooled on ice. Absorbance was measured at 470, 532, and 600 nm to calculate MDA content using the following formula:

$$\text{MDA (nmol g}^{-1}\text{ FW)} = 6.54 \times (A_{532} \times A_{600}) - 0.56 \times A_{450}$$

### *Activity of antioxidant enzymes*

To assess the activity of antioxidant enzymes, an enzyme extract was prepared by homogenizing 0.5 g of terminal leaves with 5 mL of 100 mM potassium phosphate buffer (pH 7.0) in a mortar, then centrifuged at 15,000 g for 20

min. This enzyme extract was then used to measure the activity of superoxide dismutase (SOD), ascorbate peroxidase (APX), catalase (CAT), and peroxidase (POD) enzymes, using the methods described by Kono [48], Nakano and Asada [49], Aebi et al. [50], and Pütter [51], respectively.

## Molecular analysis

### *Primer design*

Primers for *P5CS*, *P5CR*, *PDH*, *P5CDH*, *OAT* and elongation factor-1α (*TEF-1α*) genes were designed based on sequences registered in the NCBI database (Table S1) by AlleleID 7.60 software (PremierBiosoft International, Palo Alto, CA, USA) (Fig. S1). The primers used are listed in Table 2.

### *RNA extraction, DNase treatment, and cDNA synthesis*

TRIzol reagent (Life Technologies, Carlsbad, CA, USA) was used to extract total RNA. Initially, 200 mg of leaf tissue was powdered using a pestle and liquid nitrogen in a mortar. The powder was transferred to a 2 mL microtube, and 1 mL of TRIzol reagent was added. The microtube was vortexed for 1 min then kept at room temperature (RT) for 10 min. Next, 500 µL of chloroform was added to the microtube, gently inverted for 2 min, and left at RT for an additional 10 min. After this incubation period, the microtube was centrifuged at 15,000 g for 15 min at 4 °C. The supernatant (800 µL) was carefully transferred to a new 2 mL microtube, and 500 µL of cold isopropanol was added. The microtube was again kept at RT for 10 min and then centrifuged at 14,000 g for 15 min at 4 °C. The supernatant was discarded, and 500 µL of 80% ethanol was added to the precipitate to wash it. Following the RNA wash, samples were centrifuged at 12,000 g for 15 min at 4 °C. The supernatant was removed and RNA pellets were dried in an oven at 55–60 °C for 5 min. Finally, the RNA pellets were dissolved in 50 µL of DEPC-treated water. The extracted RNA was electrophoresed on a 1% agarose gel (Fig. S2) and its quantity was evaluated using a Nano-Drop 1000 spectrophotometer (Nano-Drop, Wilmington, DEL, USA). To remove genomic DNA, a DNase I Kit (Thermo Fisher Scientific, Waltham, MA, USA) was used. Specifically, 10 µL of the extracted samples was transferred to 0.2 mL microtubes. To each microtube, 2 µL of DNase I and 2 µL of reaction buffer (containing 100 mM Tris–HCl (pH 7.5), 25 mM $MgCl_2$, 1 mM $CaCl_2$) were added and total volume was made up to 20 µL with DEPC-treated water. The resulting mixture was incubated for 30 min at 37 °C in a water bath. Finally, 2 µL of EDTA (50 mM) was added to the mixture, and it was incubated for 10 min at 65 °C (this step was performed using the PCR device). To ensure the removal of genomic DNA from the samples, the PCR reaction was performed using internal reference gene primers for *TEF-1α*. The absence of an internal reference gene band on the agarose gel indicated the successful removal of DNA from the RNA samples. After confirming the absence of genomic DNA, 500 ng of RNA was utilized for cDNA synthesis using the RevertAid First-Strand cDNA Synthesis kit (Thermo Fisher Scientific).

**Table 2** Primer sequences for gene expression analysis of tobacco plants in arsenic treatments

| Gene | Sequence (5′ – 3′) | Annealing temperature (°C) |
|---|---|---|
| *P5CS* | F: AAGGAGAGGCATGAGACAGTGAT<br>R: CCAGCATAAGCAGCATACATAGCA | 65 |
| *P5CR* | F: TCCAAGCGATTCATACAAG<br>R: AACCACCTGAGTATTATTGTC | 65 |
| *OAT* | F: ACCTGAAGGCTGTTAGAGAT<br>R: ACTCCACCACCTAATGCT | 65 |
| *PDH* | F: GATCATTTGTCCGATGTCTAA<br>R: ACTTGGTCCGTTGGTATT | 62 |
| *P5CDH* | F: AGCAAGGTATGTGTTGTTATGGA<br>R: GCTAACTTCTCTGCCACTCTT | 63 |
| *TEF-1α* | F: GCTGCTGAGATGAACAAGAG<br>R: AACTTCCACAAGGCAATATCAAT | 60 |

*Abbreviations: F* forward, *OAT* Ornithine δ-aminotransferase, *P5CDH* P5C dehydrogenase, *P5CR* P5C reductase, *P5CS* $\Delta^1$-pyrroline-carboxylate synthetase, *PDH* proline dehydrogenase, *R* reverse, *TEF-1α* elongation factor-1α

### *Quantitative Real-Time PCR (qRT-PCR)*

The cDNAs obtained were diluted to a 2:5 (v/v) ratio with DEPC-treated water. The experiments were conducted using an ABI StepOne instrument (Applied Biosystems-Thermo Fisher Scientific, Waltham, MA, USA) and detected with SYBR Green. qRT-PCR was performed in a total volume of 25 µL, including 1 µL of cDNA, 1 µL of forward primer, 1 µL of reverse primer, 9.5 µL of DEPC-treated water, and 12.5 µL of SYBR Green reaction mixture (RealQ Plus Master Mix Green, AMPLIQON, Odense, Denmark). The following amplification program was used: denaturation at 95 °C for 15 min, 40 cycles of amplification at 95 °C for 30 s, annealing temperature for each gene (see Table 2) for 30 s, and 72 °C for 30 s after which a melting curve was produced at 60–95 °C. Threshold cycle (Ct) quality obtained from the device was checked and inserted into the $2^{-\Delta\Delta Ct}$ formula to calculate relative gene expression [52]. The *TEF-1α* gene was used as the internal reference gene.

## Statistical analysis

Statistical analysis was performed using SAS version 9.4 software (SAS Institute Inc., Cary, NC, USA). A one-way analysis of variance (ANOVA) was conducted to determine if there were any statistically

significant differences among treatments. The LSD test was used to determine differences between treatments at a significance level of 0.05. All morphological and physiological traits were measured as four biological replicates. The relative expression of genes was calculated using four biological and three technical replicates.

## Results

### ANOVA analysis of evaluated parameters

The ANOVA results indicate that As treatment significantly affected all measured morpho-physiological (Table S1) and biochemical (Table S2) traits, as well as the expression of genes related to proline synthesis and degradation (Table S3).

### Morphological traits

Increasing As concentration in soil significantly reduced leaf area, as well as the FW and DW of both shoots and roots (Figs. 1 and 2a-e). Control plants displayed the highest values for these traits, while the lowest values were observed in plants treated with 40 mg As $Kg^{-1}$ soil, displaying a 53.97%, 52.94%, 63%, 41.72%, and 62.14% decrease in shoot FW, shoot DW, leaf area, root FW and root DW, respectively, compared to the control (Fig. 2a-e).

### Physiological traits

#### *Photosynthetic efficiency and chlorophyll content*

When As concentration in soil increased, there was a significant decrease in photosynthetic efficiency (Fig. 2f) and chlorophyll content (Fig. 3a) in tobacco plants. The highest and lowest values of these traits were obtained in the control and 40 mg As $Kg^{-1}$ soil treatment, respectively (Figs. 2f and 3a). Photosynthetic efficiency in the 10, 20, and 40 mg As $Kg^{-1}$ soil treatments decreased by 7.55%, 17.78%, and 26.36%, respectively (Fig. 2f) while chlorophyll content decreased by 7.81%, 22.35%, and 38.43%, respectively compared to the control (Fig. 3a).

### Biochemical traits

#### *Total soluble carbohydrate, protein and proline contents*

As concentration significantly impacted the levels of total soluble carbohydrates, proteins, and proline (Fig. 3b-d). Carbohydrate and proline contents increased significantly with an increase in As concentration in soil. The highest values for both were observed when As concentration was 40 mg As $Kg^{-1}$ soil, while the lowest values were observed in control plants (Fig. 3b and d). In response to 40 mg As $Kg^{-1}$ soil, carbohydrate and proline content increased 1.7- and 4.31-fold, respectively, compared to the control (Fig. 3b and d). There was also a noticeable decline in protein content when As concentration in soil increased. Control plants exhibited the highest value, while the lowest value was observed at 40 mg As $Kg^{-1}$ soil (Fig. 3c). Protein content in the 10, 20, and 40 mg As $Kg^{-1}$ soil treatments revealed a 26.97%, 64.15%, and 78.95% decrease respectively, compared to the control (Fig. 3c).

#### *$H_2O_2$ and MDA contents*

As concentration had a significant and similar effect on $H_2O_2$ and MDA contents (Fig. 3e, f), with the highest and lowest content obtained in the 40 mg As $Kg^{-1}$ soil treatment and control, respectively (Fig. 3e, f). $H_2O_2$ content in response to 10, 20, and 40 mg As $Kg^{-1}$ soil increased 5-, 4-, and sevenfold, respectively, while MDA content increased 4-, 5-, and sevenfold, respectively compared to the control (Fig. 3e, f).

#### *Activity of antioxidant enzymes*

As concentration had a significant effect on the activity of SOD, APX, CAT, and POD (Fig. 4a-d). SOD and APX activities showed an increasing trend when As

**Fig. 1** The effect of different concentrations of arsenic on morphological traits and chlorophyll content of tobacco plants. From right to left, treatments of 0, 10, 20, and 40 mg $kg^{-1}$ soil of arsenic, respectively

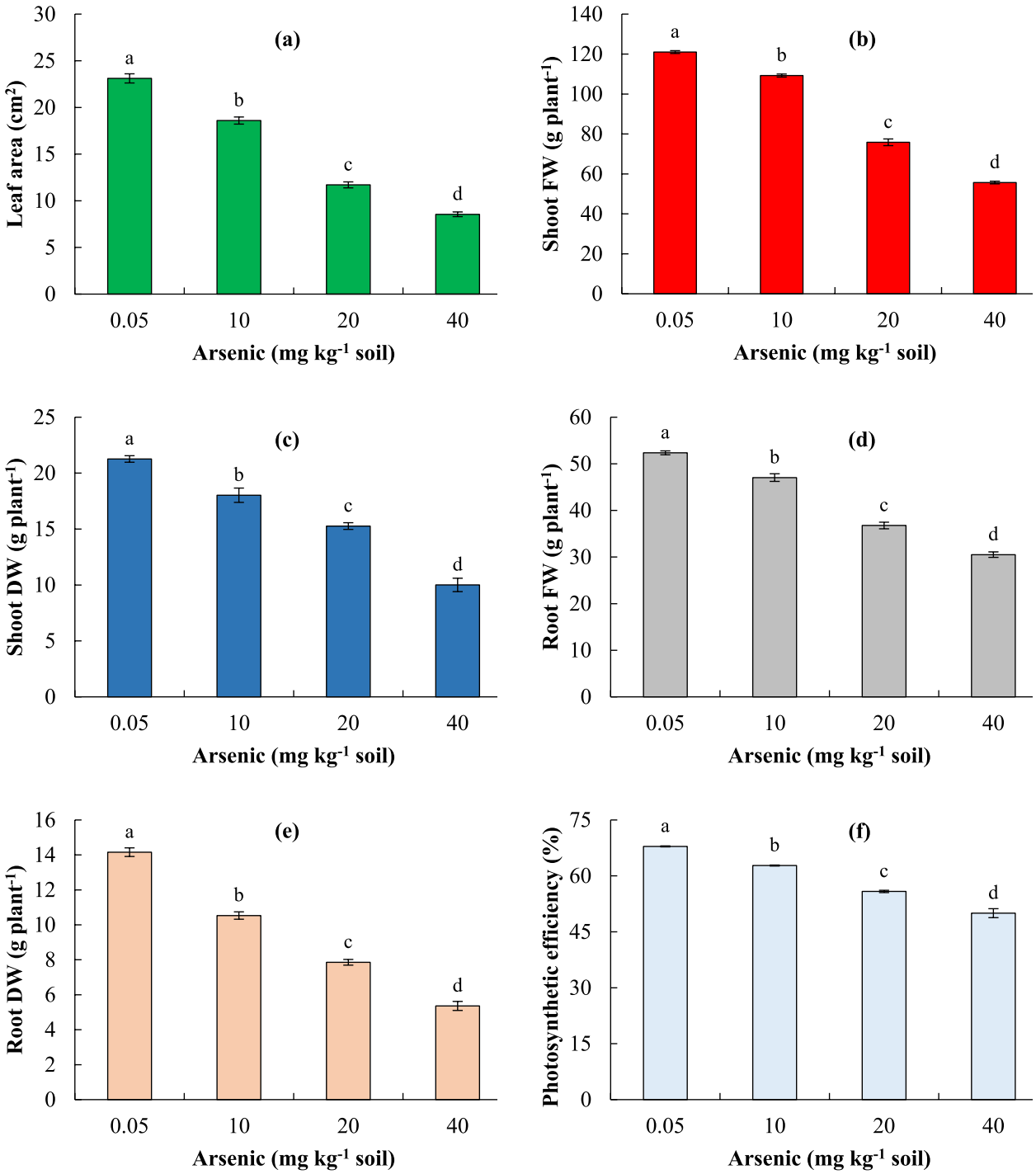


**Fig. 2** The effect of different concentrations of arsenic in soil on leaf area (**a**), shoot FW (**b**), shoot DW (**c**), root FW (**d**), root DW (**e**), and photosynthetic efficiency (**f**) in tobacco plants. The same letters above the error bars are not significantly different (LSD test; $P \leq 0.05$). Bars indicate means ± SD ($n = 4$ biological replicates). DW, dry weight; FW, fresh weight

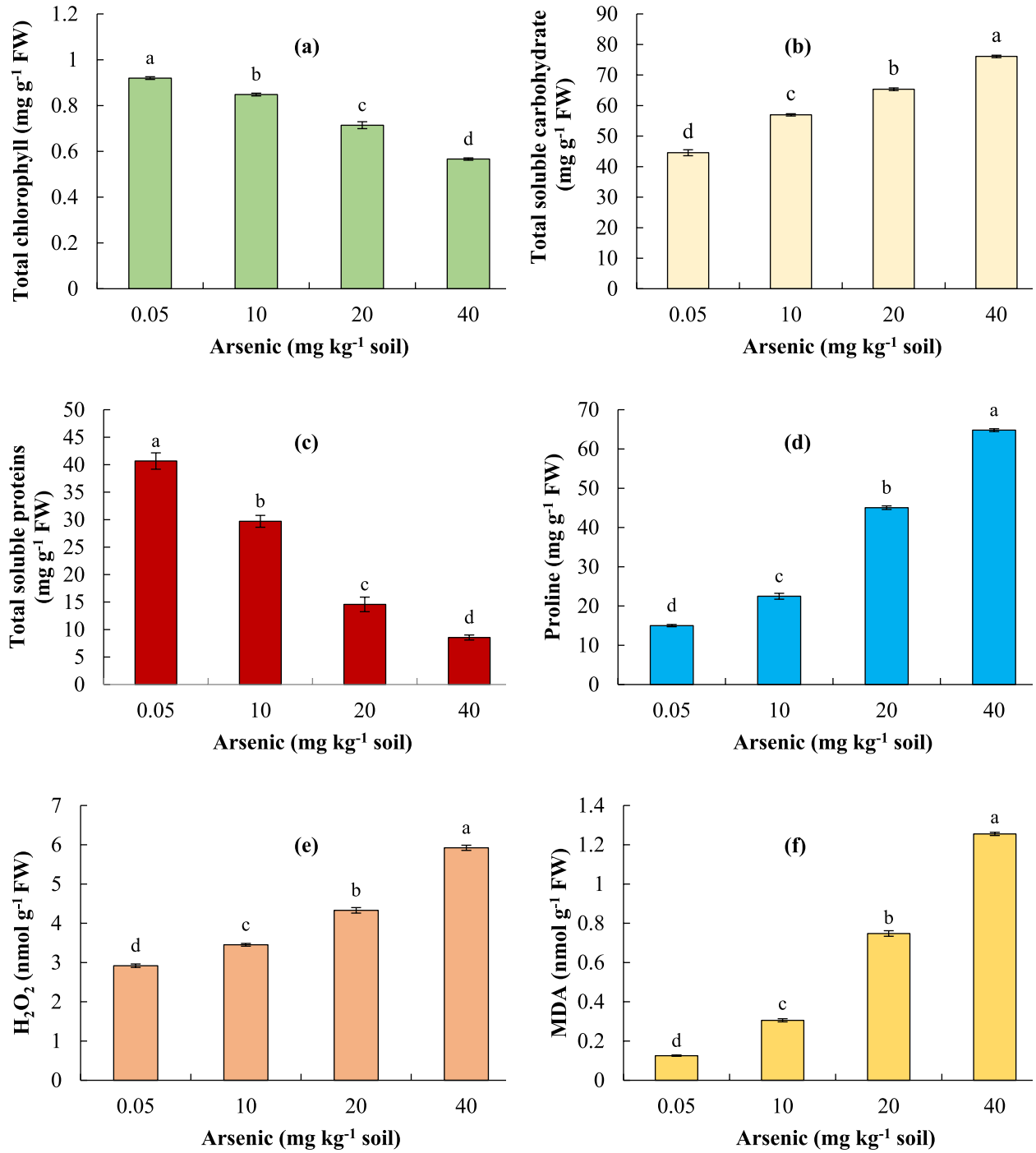


**Fig. 3** The effect of different concentrations of arsenic in soil on total chlorophyll content (**a**), total soluble carbohydrate content (**b**), total soluble proteins content (**c**), proline content (**d**), hydrogen peroxide ($H_2O_2$) content (**e**), and malondialdehyde (MDA) content (**f**) in tobacco plants. The same letters above the error bars are not significantly different (LSD test; $P \leq 0.05$). Bars indicate means ± SD ($n = 4$ biological replicates). FW, fresh weight

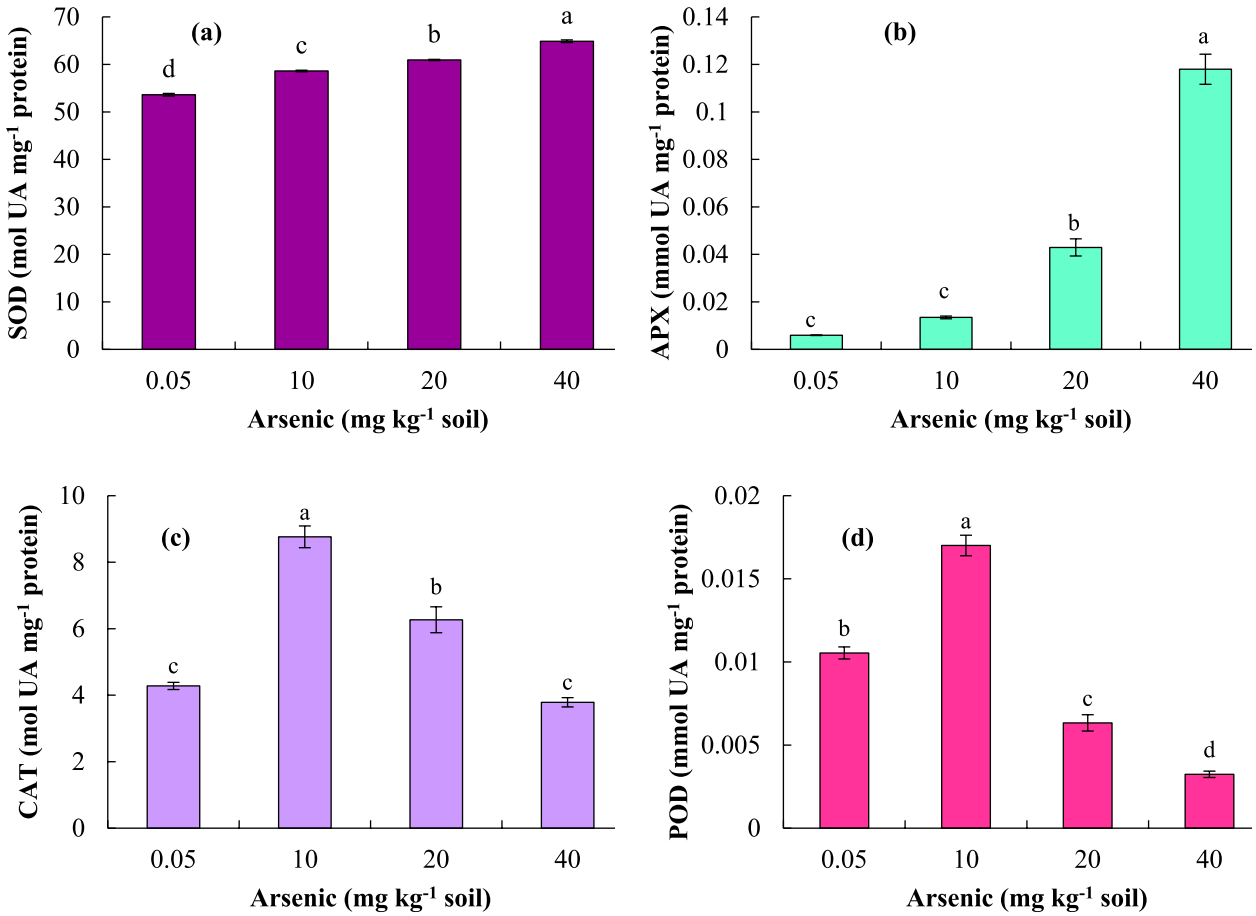


**Fig. 4** The effect of different concentrations of arsenic in soil on enzyme activity: Superoxide dismutase (SOD) (**a**), ascorbate peroxidase (APX) (**b**), catalase (CAT), (**c**) and peroxidase (POD) (**d**) in tobacco plants. The same letters above the error bars are not significantly different (LSD test; $P \leq 0.05$). Bars indicate means ± SD ($n = 4$ biological replicates)

concentration in soil increased, and the highest activity was observed at 40 mg As $Kg^{-1}$ soil (Fig. 4a, b). In addition, highest CAT and POD activities were observed at 10 mg As $Kg^{-1}$ soil, decreasing when As concentration was 20 and 40 mg As $Kg^{-1}$ soil (Fig. 4c, d).

### *Expression of genes in the proline biosynthetic pathway*

As concentration had a significant effect on the expression of genes involved in proline synthesis following the primary (*P5CS* and *P5CR*) pathway and the alternative (*OAT*) pathway (Fig. 5a-c). The expression of *P5CS* and *P5CR* genes showed a similar trend under As stress (Fig. 5a, b). The expression of these two genes in response to 10 mg As $Kg^{-1}$ soil was not significantly different from the control, but their expression increased sharply when tobacco plants were exposed to 20 and 40 mg As $Kg^{-1}$ soil. The expression of *P5CS* and *P5CR* genes increased 20.85- and 7.72-fold in the 20 mg As $Kg^{-1}$ soil treatment and 34.52- and 26.05-fold in the 40 mg As $Kg^{-1}$ soil treatment compared to the control (Fig. 5a, b). At 10 and 20 mg As $Kg^{-1}$ soil, *OAT* expression was not significantly different from the control, but its expression increased sharply (19.01-fold compared to the control) when plants were exposed to 40 mg As $Kg^{-1}$ soil (Fig. 5c).

### *Expression of genes in the proline degradation pathway*

As concentration had a significant effect on the expression of genes (*PDH* and *P5CDH*) involved in the proline degradation pathway (Fig. 5d, e). *PDH* and *P5CDH* expression showed a similar trend under As stress. In control plants, the expression of *PDH* and *P5CDH* was 29.04 and 13.06, respectively. However, in plants treated with 10 mg As $Kg^{-1}$ soil, their expression decreased to 3.2 and 2.39, respectively. Interestingly, their expression levels remained unchanged in the 20 and 40 mg As $Kg^{-1}$ soil treatments (Fig. 5d, e).

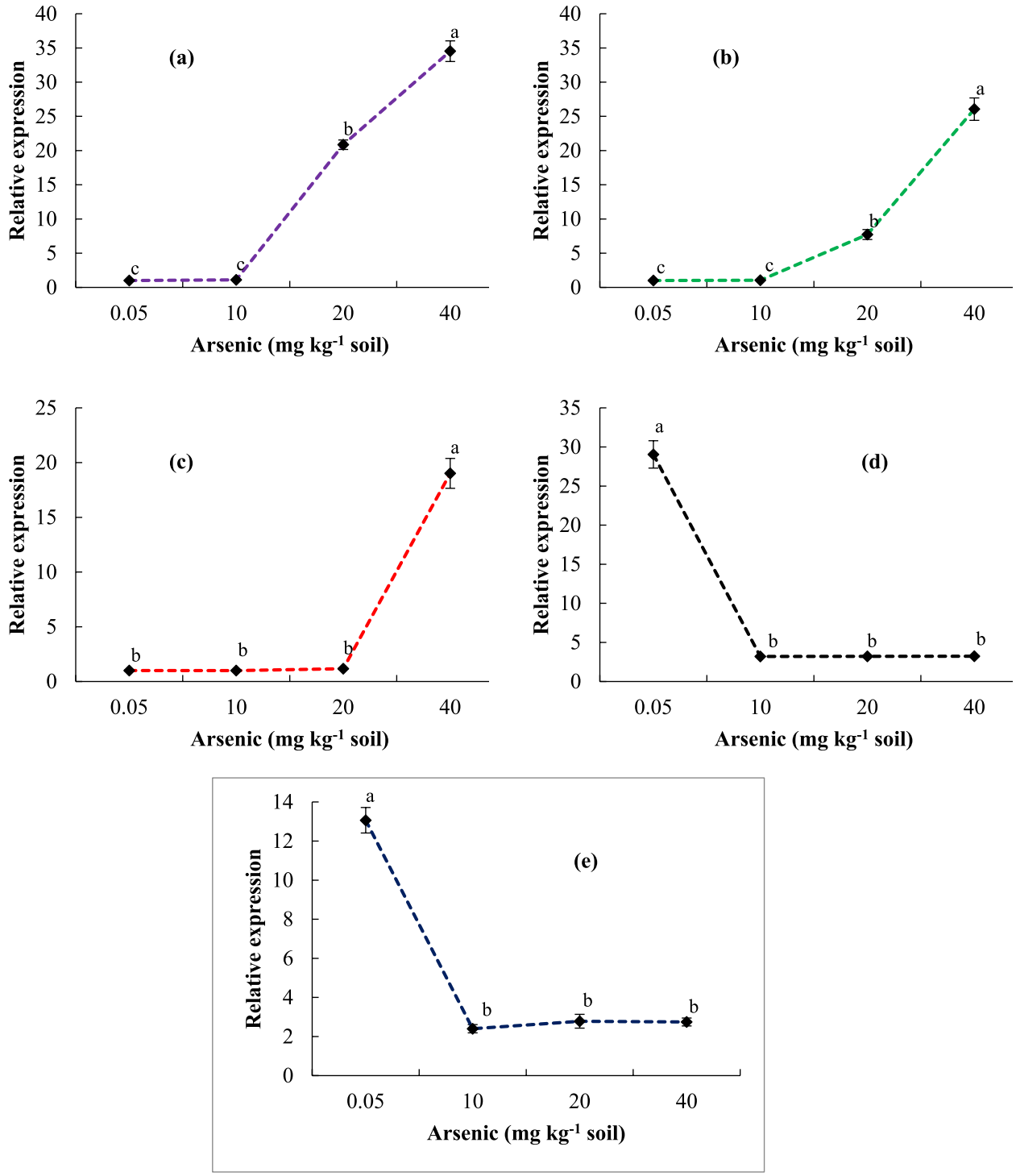


**Fig. 5** The effect of different concentrations of arsenic in soil on the expression of $\Delta^1$-pyrroline-carboxylate synthetase (*P5CS*) (**a**), P5C reductase (*P5CR*) (**b**), ornithine δ-aminotransferasegenes (*OAT*) (**c**), proline dehydrogenase (*PDH*) (**d**), and P5C dehydrogenase (*P5CDH*) (**e**) genes in tobacco plants. The same letters above the error bars are not significantly different (LSD test; $P \leq 0.05$). Bars are means ± SD ($n = 4$ biological replicates and three technical replicates)

## Discussion

The accumulation of As disrupts various physiological processes in plants, leading to inhibited growth and ultimately resulting in plant death [53]. Morphologically, As inhibits shoot and root growth, but also causes leaf chlorosis and necrosis, resulting in a decrease in leaf area and photosynthetic ability [54]. In this study, these growth indices decreased when tobacco plants were exposed to As stress (Figs. 1 and 2). Similarly, a decrease in growth characteristics such as leaf area, FW and DW of roots and shoots, and stem and root height was observed in Siberian wild rye (*Elymus sibiricus* L.) [55], bell pepper (*Capsicum annuum* L.) [56], barley (*Hordeum vulgare* L.) [57], Indian mustard (*Brassica juncea* L.) [58], and wheat [59] plants under As stress. Tobacco plants showed a decrease in root FW and DW under As stress (Fig. 2d, e). The exposure of roots to As induced the death of root cells, a decrease in the thickness of parenchyma tissue and lateral root numbers, abnormal thickening and darkening of roots, as well as necrosis of the main root apex [39, 60]. The growth of roots is inhibited by As to a greater extent than aerial organs [61], probably due to the higher accumulation of As in roots, since roots are the initial point of contact with As [61, 62]. As stress can alter the expression of genes involved in root growth, including a decrease in the expression of genes related to root apical meristem activity, which is critical for root growth and differentiation [63]. Additionally, As can disrupt energy metabolism pathways, such as NO-dependent alternate oxidase and lactate fermentation, which are essential for maintaining root growth under stress conditions [60, 64].

In tobacco shoots, As exposure resulted in a decrease in growth indices (leaf area, shoot FW and DW) (Figs. 1 and 2). Reduced plant growth under As stress has been attributed to reduced root growth and uptake and transport of nutrients [65]. As toxicity leads to nutrient imbalances, particularly affecting the availability of essential elements such as P, Fe, Zn, and Mn, and these nutrient deficiencies can impair root growth and overall plant development [63]. In addition, As can interfere with the activity of transporters involved in the absorption and transport of nutrients, further exacerbating nutrient deficiencies and impairing growth [63]. For example, due to the chemical similarity of As to phosphate, As has a high affinity with phosphate transporter 1, so its uptake by roots is facilitated and it substitutes phosphate in several cellular pathways, leading to the production of ATP, thus negatively impacting plant growth [65]. As toxicity increases the production of reactive oxygen species (ROS), whose accumulation causes oxidative damage to plant cells, with the resulting oxidative stress impairing cell function and inhibiting growth [66]. Our results showed that plant growth decreased when ROS accumulated (Figs. 1 and 3e).

Another reason for reduced growth in the presence of As stress is the decline in photosynthesis due to chlorophyll destruction and stomatal closure [67]. Under heavy metal stress, the decrease in the net rate of photosynthesis is directly associated with stomatal conductance, a reduction in the content of photosynthetic pigments, and the impaired activity of enzymes involved in $CO_2$ fixation [68, 69]. Under As stress, stomatal closure leads to $CO_2$ deprivation and arrests photosynthetic C-assimilation [70]. The high sensitivity of chlorophyll due to the toxicity of heavy metals has made it a suitable indicator for investigating the effects of heavy metal stress [70]. The decrease in chlorophyll biosynthesis has been attributed to the disruption of the thylakoid membrane and the effect of As ions in preventing the activity of rubisco, δ-aminolevulinic acid dehydratase, and protochlorophyllide reductase, which are involved in the formation of chlorophyll [60]. Our findings revealed a linear decrease in chlorophyll content when As concentration increased (Fig. 3a), with a direct negative impact on photosynthetic performance (Fig. 2f), suggesting a potential relationship with reduced plant growth. The reduction in maize (*Zea mays* L.) growth and yield under combined As and Cd stress was attributed to chlorophyll degradation, restricted $CO_2$ uptake due to impaired stomatal function, decreased activity of $CO_2$-fixing enzymes, and a subsequent decline in photosynthetic efficiency [70].

In tobacco, soluble carbohydrates accumulated when As concentration increased (Fig. 3b). Soluble carbohydrates accumulate during heavy metal stress as osmoregulators, protecting membranes and serving as a source of energy [71]. However, the accumulation of soluble carbohydrates is a response to reduced photosynthetic ability (Fig. 2f) during heavy metal stress, acting as storage reserves to carry out basic metabolism and supplying carbon for the growth and development of plants [71]. The accumulation of carbohydrates induced by As stress also provides protection against oxidative stress caused by the accumulation of free radicals, enhancing plant stress resistance [72]. As-resistant tobacco genotypes have a greater content of soluble carbohydrates [72]. In tobacco, under As stress, the production of soluble carbohydrates may have served the functions of an osmotic protector and to remove free radicals, which is associated with a decrease in the content of soluble proteins (Fig. 3c). In support of our results, a decrease in soluble proteins was observed in rice [73] and *Myriophyllum verticillatum* L. [74] plants under As stress. When carbohydrate levels are low, protein breakdown becomes a crucial source of carbon for respiration. Therefore, the typical

reduction in protein levels seen with As exposure, along with As likely lowering carbohydrate metabolism and thus hindering amino acid production, indicates that any changes in amino acid pools are probably due to amino acids being released after protein degradation [75].

Furthermore, the decrease in soluble proteins under As stress is a result of oxidative stress induced by ROS [76]. The increase of MDA and $H_2O_2$ in tobacco reflects the occurrence of oxidative stress (Fig. 3e, f). The accumulation of ROS, including $H_2O_2$, superoxide, hydroxyl, and singlet oxygen, is one of the consequences of heavy metal stress [77]. ROS can be generated by ROS-active metals by stimulating NADPH oxidases, or by inhibiting enzymes through the displacement of essential cations [78]. If the accumulation of ROS in cells exceeds their detoxification capacity, those cells will experience oxidative stress, leading to the oxidation of molecules such as DNA, proteins, and lipids [78, 79]. During As stress, the production of MDA – a result of lipid peroxidation – occurs after oxidative stress, which is caused by the excessive accumulation of ROS [80]. Our findings showed that the accumulation of $H_2O_2$ and MDA in tobacco leaves occurred in response to an increase in As concentration (Fig. 3e, f). These results show that oxidative stress occurred following the accumulation of $H_2O_2$, while the increase in MDA content indicates the oxidation of lipids and the collapse of cell membranes [60]. Plants are equipped with antioxidant enzyme defense systems such as APX, SOD, POD, and CAT, and non-enzymatic defense systems like ascorbic acid and glutathione to deal with oxidative stress [60]. Our results showed that SOD and APX activities increased when As concentration increased from 0 to 40 mg As $Kg^{-1}$ soil (Fig. 4 a, b), reaching their peak activity at 40 mg As $Kg^{-1}$ soil. However, CAT and POD activities increased at 10 mg As $Kg^{-1}$ soil, but declined at higher concentrations (Fig. 4c, d). Several studies that investigated the activities of antioxidant enzymes under As stress showed that the activities varied depending on the plant species, as well as the level and length of the stress [60]. However, in our research using tobacco, SOD and APX appeared to be effective antioxidants when dealing with As stress. An increase in SOD and APX activities was also reported in lettuce (*Lactuca sativa* L.) [81], wheat [82], and sweet wormwood (*Artemisia annua*) [83] plants under oxidative stress.

Our findings show that proline accumulation increased sharply when the concentration of As increased (Fig. 3d). Proline accumulation is a strategy to increase plant resistance when faced with heavy metal stress [84]. Proline sustains cellular osmolarity, chelates metal ions, scavenges free radicals, improves protein functions, protects the photosynthetic apparatus, allows for redox homeostasis, and stabilizes mitochondrial electron transport complex II, DNA, and protein in reaction to As [85–87]. Other plants, such as rice [85], tomato (*Solanum lycopersicum* L.) [87], pea (*Pisum sativum* L.) [88], faba bean (*Vicia faba* L.) [86], and finger millet (*Eleusine coracana* (L.) Gaertn) [89], accumulated proline in response to As stress. Plants accumulate proline under As stress via the action of enzymes involved in proline metabolism and catabolism [90]. One objective of this study was to determine the contribution of each pathway in the synthesis and degradation of proline. When As concentration was 10 mg As $Kg^{-1}$ soil, proline accumulated, and the expression of *P5CS* and *P5CR* genes did not show a significant difference relative to the control (Figs. 3d and 5a, b). However, at the same concentration, the expression of *PDH* and *P5CDH* genes implicated in proline catabolism showed a sharp decrease (Fig. 5d, e). Although the production of proline is due to an enhancement in the activities of enzymes involved in proline synthesis, as well as a simultaneous decrease in the activities of enzymes involved in proline catabolism [91], in our research, 10 mg As $Kg^{-1}$ soil decreased the enzymatic activity related to proline degradation, leading to the accumulation of proline while the enzymes implicated in proline synthesis played no role. The cause of proline accumulation in non-acclimated cucumber cell suspension cultures grown under salt stress (150 and 200 mM NaCl) was due to a reduction in the activity of PDH, an enzyme, and the role of P5CS was ineffective [92]. In tobacco, at 20 and 40 mg As $Kg^{-1}$ soil, *P5CS* and *P5CR* expression increased sharply, corresponding to an increase in proline content (Figs. 3d and 5a, b), suggesting that during As stress, the glutamate pathway was involved in proline synthesis. Under stress, the accumulation of proline is mediated through the main glutamate pathway by increasing the activity of *P5CS* and *P5CR* [93]. In agreement with our results, the expression of *P5CS* and *P5CR* genes, as well as the activity of their enzymes, has been reported under the toxicity of heavy metals such as Cr, Cd, and Pb in wheat [94], cotton (*Gossypium herbaceum* L.) [95], and tomato [96].

In contrast, in tobacco, the expression of *PDH* and *P5CDH* decreased sharply at 10 mg As $Kg^{-1}$ soil but remained unchanged at 20 and 40 mg As $Kg^{-1}$ soil (Fig. 5d, e). These results indicate that the enzymes associated with proline degradation only contributed to the increase of proline in response to a low concentration of As, but were unresponsive when As concentration was 20 and 40 mg As $Kg^{-1}$ soil. In wheat plants exposed to Cu and Cd stress, PDH activity decreased initially, but remained unchanged throughout the stress treatments, attributing the increase of proline – when PDH activity was unchanged – to an increase in P5CS and P5CR activity [97].

OAT is a crucial enzyme for the synthesis of proline and has a beneficial role in enhancing tolerance to environmental stress by promoting the augmentation of proline [98]. For example, in salinity, PEG, $H_2O_2$, and dehydration stresses, *OAT* gene expression increased, accompanied by an enhancement of proline, in grape (*Vitis vinifera* L.) [99]. In order to confirm the role of OAT in proline accumulation under stress conditions, the use of gabaculine, an inhibitor of this enzyme, was associated with a reduction in proline content under salinity stress in radish (*Raphanus sativus* L.) cotyledons [100]. In addition, other studies confirmed the role of OAT in proline accumulation under stress conditions. For example, expression of the *Arabidopsis thaliana* (L.) Heynh. *OAT*-encoded gene (*AtOAT*) in wheat improved salinity and drought stress tolerance by increasing proline content [101]. Similarly, overexpression of *AtOAT* in tobacco [102] and rice [103] increased resistance to salinity and drought stress by improving proline content. Even though several studies provide evidence of the positive role of *OAT* in improving stress tolerance through proline accumulation, some studies disprove this claim. For example, Roosens et al. [104] noted that despite the improvement of proline in 4-week-old *Arabidopsis thaliana* plants under salt stress, *OAT* gene expression was undetectable and OAT activity remained unchanged. Delauney et al. [105] observed a strong decrease in *OAT* expression in moth bean (*Vigna aconitifolia* (Jacq.) Marechal.) plants exposed to 400 mM NaCl, whereas proline accumulated. The accumulation of proline in *A. thaliana oat* mutants was not significantly different than in wild type plants under salt stress [106].

Despite many studies on the ornithine pathway, its regulatory mechanism remains unclear. In tobacco, *OAT* expression was unchanged in response to 10 and 20 mg As $Kg^{-1}$ soil compared to the control, but its expression increased significantly when As concentration was 40 mg As $Kg^{-1}$ soil (Fig. 5c), suggesting that the ornithine pathway contributed to the accumulation of proline at a high concentration of As. Activation of the ornithine pathway, and the subsequent accumulation of proline, appears to be impacted by the intensity of the stress [107]. *OAT* expression at a late stage of severe osmotic stress contributed to the amplification of proline in oilseed rape (*Brassica napus* L.) [108].

In the pathway of proline synthesis via ornithine, P5C produced by OAT is converted to glutamate by P5CDH and again enters the main proline synthesis pathway, or P5C from mitochondria enters the cytosol by carriers and is reduced to proline by P5CR [31]. Some studies reported that P5C produced by OAT is converted to glutamate by P5CDH, then re-enters the glutamate pathway. For example, Funck et al. [106] observed a high correlation between *OAT* and *P5CDH* expression in *A. thaliana*, and under salt stress, P5C derived from OAT entered the glutamate pathway via P5CDH twice. However, some studies disagree with the conversion of P5C to glutamate by P5CDH. For example, due to the suppression of the *P5CDH* gene in wheat [101], grape [99], and cashew nut (*Anacardium occidentale* L.) [109], OAT-derived P5C cannot be converted to glutamate by P5CDH and enter the glutamate pathway again; instead, P5C is transported from the mitochondria to the cytosol, where it is converted to proline by P5CR. Our findings show that *OAT* expression increased significantly at the highest concentration of As (40 mg As $Kg^{-1}$ soil) (Fig. 5c) whereas *P5CDH* expression was almost suppressed (Fig. 5e). These results indicate that OAT-derived P5C cannot be converted to glutamate by P5CDH, but instead enters the cytosol from mitochondria and is converted to proline by P5CR.

In the same context, it has been reported that in two species of rose (*Rosa* sp.) under drought, increased expression of the *OAT* gene facilitated the conversion of ornithine to P5C, but suppression of the *P5CDH* gene indicated that P5C could not be converted to glutamate and was transported from the mitochondria to the cytosol, where it was reduced to proline by P5CR [110]. More robust data would be needed to verify this supposition. One unknown underlying a clearer understanding of the ornithine pathway is the lack of identification of P5C transporters.

## Conclusion

Our findings showed that morphological traits of tobacco plants decreased under As toxicity, which may explain the destruction of chlorophyll and reduced photosynthesis. The increased level of $H_2O_2$ and MDA as two biomarkers showed that oxidative stress occurred. In response, tobacco plants activated their antioxidant system to deal with it, with SOD and APX being the most effective defense enzymes. The accumulation of proline by activation of glutamate and ornithine pathways, due to an increase in As concentration, shows that tobacco adopts a mechanism of accumulating soluble compounds to reduce the harmful effects of As stress. At a low concentration of As, the accumulation of proline was caused by a decrease in the activity of enzymes involved in proline catabolism and not the enzymes involved in its synthesis. When As concentration was 20 and 40 mg As $Kg^{-1}$ soil, the glutamate pathway played the main role in the augmentation of proline, and the increase in *OAT* expression in response to 40 mg As $Kg^{-1}$ soil indicates that the ornithine pathway was activated only at the highest concentration of As.

**Abbreviations**

| | |
|---|---|
| APX | Ascorbate peroxidase |
| As | Arsenic |
| CAT | Catalase |
| GSA | Glutamate semialdehyde |
| $H_2O_2$ | Hydrogen peroxide |
| MDA | Malondialdehyde |
| OAT | Ornithine δ-aminotransferase |
| P5C | Pyrroline-5-carboxylate |
| P5CDH | P5C dehydrogenase |
| P5CR | P5C reductase |
| P5CS | $\Delta^1$-Pyrroline-carboxylate synthetase |
| PDH | Proline dehydrogenase |
| POD | Peroxidase |
| ROS | Reactive oxygen species |
| SOD | Superoxide dismutase |

## Supplementary Information

The online version contains supplementary material available at https://doi.org/10.1186/s12870-025-06262-x.

Supplementary Material 1.

Supplementary Material 2.

**Acknowledgements**
The authors thank the Vice President for Research and Technology, University of Kurdistan, for financial support.

**Clinical trial number**
Not applicable.

**Authors' contributions**
N.A. conceptualization, designed the experiment, performed the experiment, writing – original draft; F.N. designed the experiment, supervision, writing – original draft; A.M.N. methodology, data curation, validation, software; and J.A.T.d.S. editing, provided scientific advice and guidance. All authors reviewed and approved the final version of the manuscript.

**Funding**
This research was financially supported by the University of Kurdistan (grant No. CRC97-00242–1).

**Data availability**
All data are available upon request to the corresponding author, Farzad Nazari (f.nazari@uok.ac.ir).

## Declarations

**Ethics approval and consent to participate**
This study did not include human or animal subjects.

**Consent for publication**
Not applicable.

**Competing interests**
The authors declare no competing interests.

**Author details**
[1]Department of Horticultural Science, Faculty of Agriculture, University of Kurdistan, Sanandaj, Iran. [2]Independent Researcher, Ikenobe 3011-2, Miki-cho, Kagawa-ken 761-0799, Japan.

Received: 15 October 2024 Accepted: 14 February 2025
Published online: 25 February 2025

**References**

1. Hernanda RAP, Lee H, Cho JI, Kim G, Cho BK, Kim MS. Current trends in the use of thermal imagery in assessing plant stresses: A review. Comput Electron Agric. 2024;224: 109227.
2. Huang Q, Ayyaz A, Farooq MA, Zhang K, Chen W, Hannan F, Sun Y, Shahzad K, Ali B, Zhou W. Silicon dioxide nanoparticles enhance plant growth, photosynthetic performance, and antioxidants defence machinery through suppressing chromium uptake in *Brassica napus* L. Environ Pollut. 2024;342: 123013.
3. Jomova K, Alomar SY, Nepovimova E, Kuca K, Valko M. Heavy metals: toxicity and human health effects. Arch Toxicol. 2025;99:153–209.
4. Biswas S, Ganesan M. Current perspectives of ACR3 (arsenite efflux system) toward the reduction of arsenic accumulation in plants. J Crop Sci Biotechnol. 2024;27:313–29.
5. Soini SA, Feliciano SM, Duersch BG, Merk VM. Nanocrystalline iron hydroxide lignocellulose filters for arsenate remediation. RSC Sustainability. 2024;2(3):626–34.
6. Bali AS, Sidhu GPS. Arsenic acquisition, toxicity and tolerance in plants-from physiology to remediation: A review. Chemosphere. 2021;283: 131050.
7. Nabi A, Naeem M, Aftab T, Khan MMA, Ahmad P. A comprehensive review of adaptations in plants under arsenic toxicity: Physiological, metabolic and molecular interventions. Environ Pollut. 2021;290: 118029.
8. Huang Y, Miu Q, Kwong RW, Zhang D, Fan Y, Zhou M, Yan X, Jia J, Yan B, Li C. Leveraging the One Health concept for arsenic sustainability. Eco-Environ Health. 2024;3(3):392–402.
9. Villamarín C, Loachamin M, Sosa M, Donoso M, Granda-Albuja G, Castillejo P, Ríos-Touma B. *Nectopsyche* sp (Trichoptera: Leptoceridae) sublethal effects caused by different concentrations of arsenic (As): A biochemical markers approach. Ecotoxicology. 2024;33(9):1062–73.
10. Sevak P, Pushkar B. Arsenic pollution cycle, toxicity and sustainable remediation technologies: A comprehensive review and bibliometric analysis. J Environ Manage. 2024;349: 119504.
11. Mutlu T. Distribution of toxic and trace metals in fish from the Black Sea: Implications for human health risks. Emerging Contam. 2024;10(2): 100295.
12. Ali S, Tyagi A, Mushtaq M, Al-Mahmoudi H, Bae H. Harnessing plant microbiome for mitigating arsenic toxicity in sustainable agriculture. Environ Pollut. 2022;300: 118940.
13. Shabab Z, Dronamraju SV. Modulation of quiescent center genes by 24-epibrassinolide restores root phenotype and cell wall architecture in arsenate-stressed rice seedlings. J Plant Growth Regul. 2024;43:4120–34.
14. Chandrakar V, Pandey N, Keshavkant S. Plant responses to arsenic toxicity: morphology and physiology. In: Hasanuzzaman M, Nahar K, Fujita M, editors. Mechanisms of arsenic toxicity and tolerance in plants. Springer International Publishing; 2018. p. 27–48.
15. Ejaz U, Khan SM, Khalid N, Ahmad Z, Jehangir S, Fatima Rizvi Z, Lho LH, Han H, Raposo A. Detoxifying the heavy metals: A multipronged study of tolerance strategies against heavy metals toxicity in plants. Front Plant Sci. 2023;14:1154571.
16. Zulfiqar F, Ashraf M. Proline alleviates abiotic stress induced oxidative stress in plants. J Plant Growth Regul. 2023;42(8):4629–51.
17. Saini S, Sharma P, Sharma J, Pooja P, Sharma A. Drought stress in *Lens culinaris*: Effects, tolerance mechanism, and its smart reprogramming by using modern biotechnological approaches. Physiol Mol Biol Plants. 2024;30(2):227–47.
18. Singh P, Choudhary KK, Chaudhary N, Gupta S, Sahu M, Tejaswini B, Sarkar S. Salt stress resilience in plants mediated through osmolyte accumulation and its crosstalk mechanism with phytohormones. Front Plant Sci. 2022;13:1006617.
19. Xie X, Gan L, Wang C, He T. Salt-tolerant plant growth-promoting bacteria as a versatile tool for combating salt stress in crop plants. Arch Microbiol. 2024;206(8):341.
20. Shah SH, Parrey ZA, Barwal SK, Mohammad F, Siddiqui MH. Deciphering the mechanism of action and crosstalk of brassinosteroids with other

plant growth regulators in orchestrating physio-biochemical responses in plants under salt stress. Plant Growth Regul. 2024;104:1285–306.
21. Tiwari YK. Proline as a key player in heat stress tolerance: Insights from maize. Discover Agric. 2024;2:121.
22. Altaf MM, Awan ZA, Ashraf S, Altaf MA, Zhu Z, Alsahli AA, Ahmad P. Melatonin induced reversibility of vanadium toxicity in muskmelon by regulating antioxidant defense and glyoxalase systems. J Hazard Mater. 2024;473: 134452.
23. Anas M, Saeed M, Naeem K, Shafique MA, Quraishi UM. Anatomical and ionomics investigation of bread wheat (*Triticum aestivum* L.) to decipher tolerance mechanisms under arsenic stress. J Plant Growth Regul. 2024;43:3609–25.
24. Sun M, Qiao HX, Yang T, Zhao P, Zhao JH, Luo JM, Xiong AS. Hydrogen sulfide alleviates cadmium stress in germinating carrot seeds by promoting the accumulation of proline. J Plant Physiol. 2024;303: 154357.
25. Mfarrej MFB, Javed S, Almeer R, Alsaidalani R, Kamel M, Saleem MH, Ali S. Phosphorus sources enhance barley growth and mitigate lead stress via antioxidant responses, proline metabolism, and gene expression. S Afr J Bot. 2024;174:138–51.
26. Brengi SH. Alleviation of copper stress in tomato plants using proline and melatonin in an open soilless system. Alexandria Sci Exch J. 2024;45(1):175–90.
27. Elkelish A, Alhudhaibi AM, Hossain AS, Haouala F, Alharbi BM, El-Banna MF, Rizk A, Badji A, Aljwaizea NI, Sayed AA. Alleviating chromium-induced oxidative stress in *Vigna radiata* through exogenous trehalose application: Insights into growth, photosynthetic efficiency, mineral nutrient uptake, and reactive oxygen species scavenging enzyme activity enhancement. BMC Plant Biol. 2024;24(1):460.
28. Emamverdian A, Ding Y, Mokhberdoran F, Xie Y. Heavy metal stress and some mechanisms of plant defense response. Sci World J. 2015;2015:756120. https://onlinelibrary.wiley.com/doi/10.1155/2015/756120.
29. Hosseinifard M, Stefaniak S, Ghorbani Javid M, Soltani E, Wojtyla Ł, Garnczarska M. Contribution of exogenous proline to abiotic stresses tolerance in plants: A review. Int J Mol Sci. 2022;23(9):5186.
30. Yan S, Zhan M, Liu Z, Zhang X. Insight into the transcriptional regulation of key genes involved in proline metabolism in plants under osmotic stress. Biochimie. 2024;228:8–14.
31. Alvarez ME, Savouré A, Szabados L. Proline metabolism as regulatory hub. Trends Plant Sci. 2022;27(1):39–55.
32. Mushtaq NU, Saleem S, Tahir I, Seth CS, Rehman RU. Crosstalk in proline biosynthesis regulates proline augmentation and resilience to salt stress in *Panicum miliaceum* L. Environ Exp Bot. 2024;224: 105810.
33. Margutti MP, Vilchez AC, Sosa-Alderete L, Agostini E, Villasuso AL. Lipid signaling and proline catabolism are activated in barley roots (*Hordeum vulgare* L.) during recovery from cold stress. Plant Physiol Biochem. 2024;206:108208.
34. Zhang Z, Xu P, Duan Z, Lu L, Nan Z, Zhang J. Overexpression of *P5CDH* from *Cleistogenes songorica* improves alfalfa growth performance under field drought conditions. Plant Physiol Biochem. 2024;209: 108551.
35. Zvobgo G, Hu H, Shang S, Shamsi IH, Zhang G. The effects of phosphate on arsenic uptake and toxicity alleviation in tobacco genotypes with differing arsenic tolerances. Environ Toxicol Chem. 2015;34(1):45–52.
36. Karimi N, Ghaderian SM, Maroofi H, Schat H. Analysis of arsenic in soil and vegetation of a contaminated area in Zarshuran. Int J Phytorem. 2009;12(2):159–73.
37. Nahar N, Rahman A, Nawani NN, Ghosh S, Mandal A. Phytoremediation of arsenic from the contaminated soil using transgenic tobacco plants expressing *ACR2* gene of *Arabidopsis thaliana*. J Plant Physiol. 2017;218:121–6.
38. Niazi NK, Bibi I, Fatimah A, Shahid M, Javed MT, Wang H, Ok YS, Bashir S, Murtaza B, Saqib ZA, Shakoor MB. Phosphate-assisted phytoremediation of arsenic by *Brassica napus* and *Brassica juncea*: Morphological and physiological response. Int J Phytoremediation. 2017;19(7):670–8.
39. Oller ALW, Regis S, Armendariz AL, Talano MA, Agostini E. Improving soybean growth under arsenic stress by inoculation with native arsenic-resistant bacteria. Plant Physiol Biochem. 2020;155:85–92.
40. Safari S, Nazari F, Vafaee Y, da Teixeira Silva JA. Impact of rice husk biochar on drought stress tolerance in perennial ryegrass (*Lolium perenne* L.). J Plant Growth Regul. 2023;42:810–26.
41. Langston BJ, Lincoln NK. The role of breadfruit in biocultural restoration and sustainability in Hawai'i. Sustainability. 2018;10(11):3965.
42. Lichtenthaler HK, Buschmann C. Extraction of photosynthetic tissues, chlorophylls and carotenoids. Food Anal Chem. 2001;1(1):F4.2.1–F4.2.6.
43. Irigoyen JJ, Einerich DW, Sánchez-Díaz M. Water stress induced changes in concentrations of proline and total soluble sugars in nodulated alfalfa (*Medicago sativa*) plants. Physiol Plant. 1992;1:55–60.
44. Bradford MM. A rapid and sensitive method for the quantitation of microgram quantities of protein utilizing the principle of protein-dye binding. Anal Biochem. 1976;72(1–2):248–54.
45. Bates LS, Waldren RA, Teare ID. Rapid determination of free proline for water-stress studies. Plant Soil. 1973;39:205–7.
46. Cui XH, Murthy HN, Wu CH, Paek KY. Sucrose-induced osmotic stress affects biomass, metabolite, and antioxidant levels in root suspension cultures of *Hypericum perforatum* L. Plant Cell Tissue Organ Cult. 2010;103:7–14.
47. Li HS, Sun Q, Zhao SJ, Zhang WH. Principles and techniques of plant physiological biochemical experiment. Higher Education, Beijing. 2000;195–197.
48. Kono Y. Generation of superoxide radical during autoxidation of hydroxylamine and an assay for superoxide dismutase. Arch Biochem Biophys. 1978;186(1):189–95.
49. Nakano Y, Asada K. Hydrogen peroxide is scavenged by ascorbate-specific peroxidase in spinach chloroplasts. Plant Cell Physiol. 1981;22(5):867–80.
50. Aebi H. Catalase in vitro Methods Enzym. 1984;105:121–6.
51. Pütter J. Peroxidases Methods Enzymatic Anal. 1974;2:685–90.
52. Livak KJ, Schmittgen TD. Analysis of relative gene expression data using real-time quantitative PCR and the $2^{-\Delta\Delta CT}$ method. Methods. 2001;25:402–8.
53. Sinha D, Datta S, Mishra R, Agarwal P, Kumari T, Adeyemi SB, Maurya AK, Ganguly S, Atique U, Seal S, Gupta LK, Chowdhury S, Chen JT. Negative impacts of arsenic on plants and mitigation strategies. Plants. 2023;12(9):1815.
54. Emamverdian A, Ding Y, Hasanuzzaman M, Barker J, Liu G, Li Y, Mokhberdoran F. Insight into the biochemical and physiological mechanisms of nanoparticles-induced arsenic tolerance in bamboo. Front Plant Sci. 2023;14:1121886.
55. Gatasheh MK, Shah AA, Kaleem M, Usman S, Shaffique S. Application of CuNPs and AMF alleviates arsenic stress by encompassing reduced arsenic uptake through metabolomics and ionomics alterations in *Elymus sibiricus*. BMC Plant Biol. 2024;24(1):667.
56. Nawaz M, Shahzadi E, Yaseen A, Khalid MR, Saleem MH, Alalawy AI, Omran AME, Khalil FMA, Alsuwat MA, Ercisli S, Malik T, Ali B. Selenium improved arsenic toxicity tolerance in two bell pepper (*Capsicum annuum* L.) varieties by modulating growth, ion uptake, photosynthesis, and antioxidant profile. BMC Plant Biol. 2024;24(1):799.
57. Alhaithloul HAS, Alghanem SMS, Alsudays IM, Abbas ZK, Al-Balawi SM, Ali B, Malik T, Javad S, Ali S, Ercisli S, Darwish DBE. Ameliorating arsenic and PVC microplastic stress in barley (*Hordeum vulgare* L.) using copper oxide nanoparticles: an environmental bioremediation approach. BMC Plant Biol. 2024;24(1):985.
58. Ahmad A, Khan WU, Shah AA, Yasin NA, Naz S, Ali A, Batool AI. Synergistic effects of nitric oxide and silicon on promoting plant growth, oxidative stress tolerance and reduction of arsenic uptake in *Brassica juncea*. Chemosphere. 2021;262: 128384.
59. Ahmad Z, Younis R, Ahmad T, Iqbal MA, Artyszak A, Alzahrani YM, Alharby HF, Alsamadany H. Modulating physiological and antioxidant responses in wheat cultivars via foliar application of silicon nanoparticles (SiNPs) under arsenic stress conditions. SILICON. 2024;16(12):5199–211.
60. Nahar K, Rhaman MS, Parvin K, Bardhan K, Marques DN, García-Caparrós P, Hasanuzzaman M. Arsenic-induced oxidative stress and antioxidant defense in plants. Stresses. 2022;2(2):179–209.
61. Kaya C, Ashraf M, Alyemeni MN, Rinklebe J, Ahmad P. Alleviation of arsenic toxicity in pepper plants by aminolevulinic acid and heme through modulating its sequestration and distribution within cell organelles. Environ Pollut. 2023;330: 121747.
62. Mishra S, Mattusch J, Wennrich R. Accumulation and transformation of inorganic and organic arsenic in rice and role of thiol-complexation to restrict their translocation to shoot. Sci Rep. 2017;7(1):40522.

63. Kumar V, Vogelsang L, Schmidt RR, Sharma SS, Seidel T, Dietz KJ. Remodeling of root growth under combined arsenic and hypoxia stress is linked to nutrient deprivation. Front Plant Sci. 2020;11: 569687.
64. Demircan N, Cucun G, Uzilday B. Mitochondrial alternative oxidase (AOX1a) is required for the mitigation of arsenic-induced oxidative stress in *Arabidopsis thaliana*. Plant Biotechnol Rep. 2020;14(2):235–45.
65. Martínez-Castillo JI, Saldaña-Robles A, Ozuna C. Arsenic stress in plants: A metabolomic perspective. Plant Stress. 2022;3: 100055.
66. Elbasan F, Arikan B, Ozfidan-Konakci C, Tofan A, Yildiztugay E. Hesperidin and chlorogenic acid mitigate arsenic-induced oxidative stress via redox regulation, photosystems-related gene expression, and antioxidant efficiency in the chloroplasts of *Zea mays*. Plant Physiol Biochem. 2024;208: 108445.
67. Rajendran S, Rathinam V, Sharma A, Vallinayagam S, Muthusamy M. Arsenic and environment: a systematic review on arsenic sources, uptake mechanism in plants, health hazards and remediation strategies. Top Catal. 2024;67(1):325–41.
68. Feki K, Tounsi S, Mrabet M, Mhadhbi H, Brini F. Recent advances in physiological and molecular mechanisms of heavy metal accumulation in plants. Environ Sci Pollut Res. 2021;28:64976–86.
69. Hu Z, Zhao C, Li Q, Feng Y, Zhang X, Lu Y, Ying R, Yin A, Ji W. Heavy metals can affect plant morphology and limit plant growth and photosynthesis processes. Agronomy. 2023;13(10):2601.
70. Anjum SA, Tanveer M, Hussain S, Ashraf U, Khan I, Wang L. Alteration in growth, leaf gas exchange, and photosynthetic pigments of maize plants under combined cadmium and arsenic stress. Water Air Soil Pollut. 2017;228:1–12.
71. Majumder B, Das S, Biswas S, Mazumdar A, Biswas AK. Differential responses of photosynthetic parameters and its influence on carbohydrate metabolism in some contrasting rice (*Oryza sativa* L.) genotypes under arsenate stress. Ecotoxicol. 2020;29:912–31.
72. Kofroňová M, Hrdinová A, Mašková P, Tremlová J, Soudek P, Petrová Š, Pinkas D, Lipavská H. Multi-component antioxidative system and robust carbohydrate status, the essence of plant arsenic tolerance. Antioxidants. 2020;9(4):283.
73. Faizan M, Sehar S, Rajput VD, Faraz A, Afzal S, Minkina T, Sushkova S, Adil MF, Yu F, Alatar AA, Akhter F, Faisal M. Modulation of cellular redox status and antioxidant defense system after synergistic application of zinc oxide nanoparticles and salicylic acid in rice (*Oryza sativa*) plant under arsenic stress. Plants. 2021;10(11):2254.
74. Li J, Liu W, Lian Y, Shi R, Wang Q, Zeb A. Single and combined toxicity of polystyrene nanoplastics and arsenic on submerged plant *Myriophyllum verticillatum* L. Plant Physiol Biochem. 2023;194:513–23.
75. Finnegan PM, Chen W. Arsenic toxicity: The effects on plant metabolism. Front Physiol. 2012;3:182.
76. Siddiqui MH, Alamri S, Khan MN, Corpas FJ, Al-Amri AA, Alsubaie QD, Ali HM, Kalaji HM, Ahmad P. Melatonin and calcium function synergistically to promote the resilience through ROS metabolism under arsenic-induced stress. J Hazard Mater. 2020;398: 122882.
77. Ucar S, Yaprak E, Yigider E, Kasapoglu AG, Oner BM, Ilhan E, Aydin M. Genome-wide analysis of miR172-mediated response to heavy metal stress in chickpea (*Cicer arietinum* L.): Physiological, biochemical, and molecular insights. BMC Plant Biol. 2024;24:1063.
78. Berni R, Luyckx M, Xu X, Legay S, Sergeant K, Hausman JF, Guerriero G. Reactive oxygen species and heavy metal stress in plants: Impact on the cell wall and secondary metabolism. Environ Exp Bot. 2019;161:98–106.
79. Krishnamurthy HK, Pereira M, Rajavelu I, Jayaraman V, Krishna K, Wang T, Bei K, Rajasekaran JJ. Oxidative stress: Fundamentals and advances in quantification techniques. Front Chem. 2024;12:1470458.
80. Waheed Z, Iqbal S, Irfan M, Jabeen K, Umar A, Aljowaie RM, Almutairi SM, Gancarz M. *Pseudochrobactrum asaccharolyticum* mitigates arsenic induced oxidative stress of maize plant by enhancing water status and antioxidant defense system. BMC Plant Biol. 2024;24:832.
81. Song Y, Zhang F, Li H, Qiu B, Gao Y, Cui D, Yang Z. Antioxidant defense system in lettuces tissues upon various as species exposure. J Hazard Mater. 2020;399: 123003.
82. Qin C, Lian H, Zhang B, He Z, Alsahli AA, Ahanger MA. Synergistic influence of selenium and silicon supplementation prevents the oxidative effects of arsenic stress in wheat. J Hazard Mater. 2024;465: 133304.
83. Naeem M, Aftab T, Ansari AA, Khan MMA. Carrageenan oligomers and salicylic acid act in tandem to escalate artemisinin production by suppressing arsenic uptake and oxidative stress in sweet wormwood (*Artemisia annua*) cultivated in high arsenic soil. Environ Sci Pollut Res. 2021;28:42706–21.
84. Yuan Z, Cai S, Yan C, Rao S, Cheng S, Xu F, Liu X. Research progress on the physiological mechanism by which selenium alleviates heavy metal stress in plants: a review. Agronomy. 2024;14(8):1787.
85. Majumder B, Das S, Mukhopadhyay S, Biswas AK. Identification of arsenic-tolerant and arsenic-sensitive rice (*Oryza sativa* L.) cultivars on the basis of arsenic accumulation assisted stress perception, morpho-biochemical responses, and alteration in genomic template stability. Protoplasma. 2019;256:193–211.
86. Ahmad P, Alam P, Balawi TH, Altalayan FH, Ahanger MA, Ashraf M. Sodium nitroprusside (SNP) improves tolerance to arsenic (As) toxicity in *Vicia faba* through the modifications of biochemical attributes, antioxidants, ascorbate-glutathione cycle and glyoxalase cycle. Chemosphere. 2020;244: 125480.
87. Ghorbani A, Pishkar L, Roodbari N, Pehlivan N, Wu C. Nitric oxide could allay arsenic phytotoxicity in tomato (*Solanum lycopersicum* L.) by modulating photosynthetic pigments, phytochelatin metabolism, molecular redox status and arsenic sequestration. Plant Physiol Biochem. 2021;167:337–48.
88. Alsahli AA, Bhat JA, Alyemeni MN, Ashraf M, Ahmad P. Hydrogen sulfide ($H_2S$) mitigates arsenic (As)-induced toxicity in pea (*Pisum sativum* L.) plants by regulating osmoregulation, antioxidant defense system, ascorbate glutathione cycle and glyoxalase system. J Plant Growth Regul. 2021;40:2515–31.
89. Rakkammal K, Pandian S, Ramesh M. Physiological and biochemical response of finger millet plants exposed to arsenic and nickel stress. Plant Stress. 2024;11: 100389.
90. Singh V, Tripathi BN, Sharma V. Interaction of Mg with heavy metals (Cu, Cd) in *Triticum aestivum* with special reference to oxidative and proline metabolism. J Plant Res. 2016;129:487–97.
91. Liu Y, Wang L, Li Y, Li X, Zhang J. Proline metabolism-related gene expression in four potato genotypes in response to drought stress. Biol Plant. 2019;63:757–64.
92. Naliwajski MR, Skłodowska M. Proline and its metabolism enzymes in cucumber cell cultures during acclimation to salinity. Protoplasma. 2014;251:201–9.
93. Luo Q, Ma Y, Xie H, Chang F, Guan C, Yang B, Ma Y. Proline metabolism in response to climate extremes in hairgrass. Plants. 2024;13(10):1408.
94. Shavalikohshori O, Zalaghi R, Sorkheh K, Enaytizamir N. The expression of proline production/degradation genes under salinity and cadmium stresses in *Triticum aestivum* inoculated with *Pseudomonas* sp. Int J Environ Sci Technol. 2020;17:2233–42.
95. Zhou B, Zhang T, Wang F. Unravelling the molecular and biochemical responses in cotton plants to biochar and biofertilizer amendments for Pb toxicity mitigation. Environ Sci Pollut Res. 2023;30(45):100799–813.
96. Shah T, Khan Z, Alahmadi TA, Imran A, Asad M, Khan SR, Ansari MJ. Mycorrhizosphere bacteria inhibit chromium uptake and phytotoxicity by regulating proline metabolism, antioxidant defense system, and aquaporin gene expression in tomato. Environ Sci Pollut Res. 2024;31(17):24836–50.
97. Tripathi BN, Singh V, Ezaki B, Sharma V, Gaur JP. Mechanism of Cu-and Cd-induced proline hyperaccumulation in *Triticum aestivum* (wheat). J Plant Growth Regul. 2013;32:799–808.
98. Arabia S, Shah MNA, Sami AA, Ghosh A, Islam T. Identification and expression profiling of proline metabolizing genes in *Arabidopsis thaliana* and *Oryza sativa* to reveal their stress-specific transcript alteration. Physiol Mol Biol Plants. 2021;27(7):1469–85.
99. Wei TL, Wang ZX, He YF, Xue S, Zhang SQ, Pei MS, Liu HN, Yu YH, Guo DL. Proline synthesis and catabolism-related genes synergistically regulate proline accumulation in response to abiotic stresses in grapevines. Sci Hortic. 2022;305: 111373.
100. Anwar A, She M, Wang K, Riaz B, Ye X. Biological roles of ornithine aminotransferase (OAT) in plant stress tolerance: present progress and future perspectives. Int J Mol Sci. 2018;19(11):3681.
101. Anwar A, Wang K, Wang J, Shi L, Du L, Ye X. Expression of *Arabidopsis* ornithine aminotransferase (*AtOAT*) encoded gene enhances multiple abiotic stress tolerances in wheat. Plant Cell Rep. 2021;40(7):1155–70.

102. Roosens NH, Bitar FA, Loenders K, Angenon G, Jacobs M. Overexpression of ornithine-δ-aminotransferase increases proline biosynthesis and confers osmotolerance in transgenic plants. Mol Plant Breed. 2002;9:73–80.
103. Wu L, Fan Z, Guo L, Li Y, Zhang W, Qu LJ, Chen Z. Over-expression of an Arabidopsis δ-OAT gene enhances salt and drought tolerance in transgenic rice. Chin Sci Bull. 2003;48:2594–600.
104. Roosens NH, Thu TT, Iskandar HM, Jacobs M. Isolation of the ornithine-δ-aminotransferase cDNA and effect of salt stress on its expression in *Arabidopsis thaliana*. Plant Physiol. 1998;117(1):263–71.
105. Delauney AJ, Hu CA, Kishor PB, Verma DP. Cloning of ornithine delta-aminotransferase cDNA from *Vigna aconitifolia* by trans-complementation in *Escherichia coli* and regulation of proline biosynthesis. J Biol Chem. 1993;268(25):18673–8.
106. Funck D, Stadelhofer B, Koch W. Ornithine-δ-aminotransferase is essential for arginine catabolism but not for proline biosynthesis. BMC Plant Biol. 2008;8:1–14.
107. Spormann S, Nadais P, Sousa F, Pinto M, Martins M, Sousa B, Fidalgo F, Soares C. Accumulation of proline in plants under contaminated soils—are we on the same page? Antioxidants. 2023;12(3):666.
108. Xue X, Liu A, Hua X. Proline accumulation and transcriptional regulation of proline biosynthesis and degradation in *Brassica napus*. BMC Rep. 2009;42(1):28–34.
109. da Rocha IMA, Vitorello VA, Silva JS, Ferreira-Silva SL, Viégas RA, Silva EN, Silveira JAG. Exogenous ornithine is an effective precursor and the δ-ornithine amino transferase pathway contributes to proline accumulation under high N recycling in salt-stressed cashew leaves. J Plant Physiol. 2012;169(1):41–9.
110. Adamipour N, Khosh-Khui M, Salehi H, Razi H, Karami A, Moghadam A. Metabolic and genes expression analyses involved in proline metabolism of two rose species under drought stress. Plant Physiol Biochem. 2020;155:105–13.


## Publisher's Note